

# Silicon nitride films deposited at substrate temperatures <100 °C in a permanent magnet electron cyclotron resonance plasma

C. Doughty,<sup>a)</sup> D. C. Knick, J. B. Bailey, and J. E. Spencer  
*PlasmaQuest, Inc., Dallas, Texas 75243*

(Received 4 June 1998; accepted 30 April 1999)

Deposition of silicon nitride at low temperatures by plasma-enhanced chemical vapor deposition requires an efficient source of activated precursors and high-current, low-energy ion assist. We report the deposition of silicon nitride at substrate temperatures <100 °C using a permanent magnet electron cyclotron resonance plasma reactor capable of generating uniform plasmas over 300 mm diameters. The effects of gas mixture, silane flow, pressure, and microwave power on the film deposition rate, composition and bonding, index of refraction, stress, and etch rate in buffered oxide etch solution are reported. The N<sub>2</sub>/SiH<sub>4</sub> flow ratio and microwave power both influence the film index and hydrogen content and bonding. For a SiH<sub>4</sub> flow of 30 sccm and N<sub>2</sub>/SiH<sub>4</sub> ~0.75, hydrogen is equally distributed between Si-H and N-H sites and total hydrogen content is minimized. At a deposition rate of 500–600 Å/min, a threshold in microwave power of ~1100 W exists, above which films with buffered oxide etch rates <150 Å/min result. Near the threshold microwave power compressive stress <400 MPa is observed, with increasing stress at higher microwave powers.  
© 1999 American Vacuum Society. [S0734-2101(99)05005-8]

## I. INTRODUCTION

Plasma-enhanced chemical vapor deposition (PECVD) is widely used to deposit thin films at lower temperatures than thermal processes. PECVD silicon nitride, variably referred to as *a*-SiN, SiN<sub>x</sub>, or SiN:H is typically deposited in a parallel plate radio frequency (rf) plasma.<sup>1</sup> The plasma enables deposition at lower temperatures than the ~800–1000 °C required for thermal CVD, however, a substrate temperature ~350–400 °C is still required to produce a dense film with minimal hydrogen content.<sup>1</sup>

For silicon integrated circuit applications ~350 °C is considered “low temperature.” A large body of other applications and materials exist for which this constitutes an unacceptably high substrate temperature. These include passivation of polymeric materials<sup>2</sup> and low-curie-temperature materials such as (PbZr)TiO<sub>3</sub>, as well as lift-off processes involving photoresist. For these applications substrate temperatures <100 °C may be required.

Silicon, silicon nitride, and silicon oxide films have been deposited at temperatures <300 °C in downstream plasma reactors<sup>3,4</sup> conventional RF-PECVD systems,<sup>5</sup> as well as divergent field electromagnet<sup>6,7</sup> and distributed electron cyclotron resonance (ECR) configurations.<sup>8</sup> Lower temperature tends to lead to higher H content and lower density, however.

High-density plasma sources such as ECRs, helicons, helical resonators, and rf-inductive sources offer a number of potential advantages in low-temperature deposition. These sources generate much higher ion densities than parallel plate rf systems, ~10<sup>11</sup>–10<sup>12</sup>/cm<sup>3</sup> compared to 10<sup>9</sup>–10<sup>10</sup>/cm<sup>3</sup>. This leads to larger ion currents to the wafer during deposition and enhanced ion assist. High-density plasma sources also produce a lower mean ion energy than capaci-

tively coupled systems, ~10–50 vs >100 eV. This energy regime may be more effective for ion-assisted deposition.<sup>9</sup> High-density sources more efficiently dissociate source gases. Conventional rf-PECVD systems must use NH<sub>3</sub> as a source of nitrogen. In contrast, high-density plasma sources can effectively dissociate N<sub>2</sub>, reducing the H content of the film.

This article reports the deposition of silicon nitride films at substrate temperatures <100 °C using a permanent magnet ECR plasma deposition system. The use of a permanent magnet to provide the magnetic field required for ECR microwave absorption leads to fundamental differences between this system and conventional divergent-field electromagnet systems. The basic system geometry also differs from other high-density plasma reactors. These differences are discussed in Sec. II, while Sec. III reports the fundamental relationships between film properties and process parameters.

## II. DEPOSITION SYSTEM

The PlasmaQuest Series III permanent magnet ECR reactor used for this work is shown schematically in Fig. 1(a). The 50 cm diam chamber is surrounded by permanent magnets forming a multipolar magnetic bucket. The system is pumped by a 2200 l/s turbomolecular pump mounted on axis below a 325 mm diam, rf-biased, fluid-cooled chuck. Samples are load-locked into the reactor on an aluminum pallet, allowing for a wide variety of samples to be easily loaded.

ECR requires a magnetic field of 875 G at the microwave excitation frequency used here, 2.45 GHz. In contrast to conventional electromagnet ECR sources, here the field is generated by a permanent magnet located at the top of the chamber.<sup>10</sup> Microwaves are absorbed in a thin disk-shaped region near the microwave window at the top of the cham-

<sup>a)</sup>Electronic mail: cdoughty@plasmaquest.com

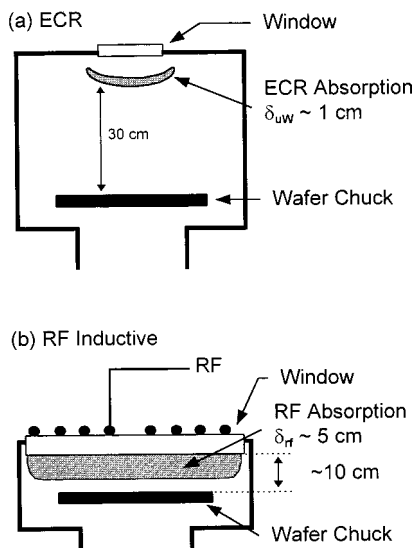


FIG. 1. Schematic of (a) permanent magnet ECR plasma deposition system and (b) typical inductively coupled system with planar coil. The ECR system has a compact region of plasma generation separated from the wafer by multiple mean-free paths.

ber. In this absorption region the plasma density exceeds  $10^{12}/\text{cm}^3$  resulting in highly efficient dissociation of molecular gases. The thickness of this region,  $\delta_{uw}$ , is  $\sim 1$  cm and the diameter  $\sim 15$  cm.<sup>11</sup> The plasma expands into the chamber and wall losses are reduced by multipolar magnetic confinement. The plasma density is  $>1 \times 10^{11}/\text{cm}^3$  at the wafer.

This system differs from other high-density plasma reactors in that the region of highest plasma density is separated from the wafer by multiple mean-free paths. At the typical operating pressure of  $\sim 5$  mTorr the mean-free path is  $\sim 1$  cm, while the separation between the absorption region and the wafer is  $\sim 30$  cm.

The situation is fundamentally different in many other high-density plasma reactors. Figure 1(b) shows a schematic of an inductively coupled plasma reactor in which a rf-driven coil is inductively coupled to the plasma across a dielectric window. The rf power is absorbed over a length scale  $\delta_{rf}$ , the rf skin depth. At typical plasma densities and 13.56 MHz,  $\delta_{rf} \sim 5$ –20 cm.<sup>12</sup> The induction coil is typically close-coupled to the substrate ( $\sim 10$ –15 cm). In terms of the mean-free path of the system, the region of plasma generation is much closer to the substrate than in the ECR system and there is no potential for spatial separation.

The separation of the microwave absorption region and the wafer allows independent control of dissociation and activation of multiple precursors. Because the system is operating in a transition flow regime and the regions are separated by multiple mean-free paths, the gas composition in the two regions can vary. In this case nitrogen is injected into the absorption region and silane into the wafer region.

The equilibrium plasma density and electron energy distribution are intimately related to the gas composition. In the case of silicon nitride CVD, silane is easily dissociated (SiH<sub>3</sub>-H, SiH<sub>2</sub>-H, SiH-H, and Si-H bond energies all  $<4$  eV) while nitrogen is much more difficult to dissociate (9.1

eV).<sup>12,13</sup> When both silane and nitrogen are present, power will predominantly flow into dissociation and activation of silane and not into activation of nitrogen. With nitrogen injected near the resonance zone in Fig. 1(a), the plasma near the resonance zone is dominated by N<sub>2</sub> which can be effectively dissociated by the high plasma density in that region. Silane injected downstream can still be activated by the somewhat lower plasma density in that region.

The spatial separation of silane and nitrogen is observed in varying deposition rates and deposition patterns within the reactor. With silane injected into the ECR zone an optically dense (presumably silicon rich) film quickly deposits on the microwave window. When silane is injected downstream, the film deposited on the chamber walls is thickest below the plane of the silane injectors. Depending on the exact point of silane injection, the N<sub>2</sub> flow injected upstream, and the pressure and flow regime, this deposit can be localized to the bottom half of the chamber, qualitatively confirming the spatial separation of silane and nitrogen in the system.

Ion-assisted deposition techniques are used in low temperature deposition to drive chemical reactions and densify the film as substrate temperatures  $<100^\circ\text{C}$  provide very little thermal energy to drive chemical reactions at the growth surface. The high current of relatively low-energy ions ( $\sim 10$ –20 V) provided by a high-density plasma is ideal for providing this plasma assist. Uniform deposition over large areas requires a uniform plasma and ion current density at the wafer.

Conventional divergent magnetic field electromagnet ECR sources<sup>12</sup> are capable of providing ion currents  $\sim 10$ –20 mA/cm<sup>2</sup> to the wafer surface during processing.<sup>11</sup> This is due to both the high plasma density generated in the resonance zone, and to efficient plasma extraction down the magnetic field lines connecting the resonance zone and the wafer. These sources have several drawbacks, however. First, the electromagnets are expensive and bulky, especially for larger diameters. Second, it has proven difficult to scale these sources to diameters greater than 200 mm. This is primarily due to the large magnetic fields coupling the resonance zone and wafer. These fields inhibit diffusion perpendicular to the field lines so that nonuniformities in the resonance zone are translated down the field lines to the wafer plane.

The system used for this work utilizes a permanent magnet to provide the magnetic field for ECR resonance, and is engineered to have a much lower field at the wafer plane than an electromagnet system. When configured for ion extraction, an electromagnet system would have a field of several hundred Gauss at the wafer plane. In the present system the field is  $<50$  G. This low magnetic field enhances diffusion perpendicular to the magnetic field lines and improves uniformity.<sup>14</sup> The permanent magnet also is substantially less complex and costly, a substantial advantage for production applications.

The uniformity of the plasma generated by this source was characterized by scanning Langmuir probe measurements. The plasma parameters were derived from measurements of the current,  $I$ , as a function of voltage,  $V$ , drawn by

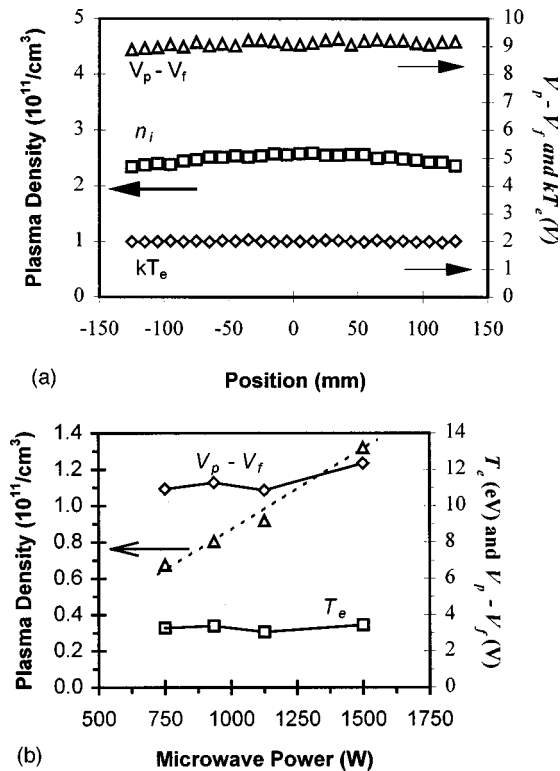


Fig. 2. (a) Dependence of plasma parameters on position in an Ar plasma at 3 mTorr and 2000 W microwave power. (b) Plasma parameters as a function of microwave power for a 5%  $\text{N}_2$  in Ar plasma at 4 mTorr.

a Langmuir probe (Scientific Systems Smart Probe) inserted into an Ar plasma. The plasma potential,  $V_p$ , and floating potential,  $V_f$ , were obtained from the intersection of the slopes above and below the electron saturation current (the knee in the  $I-V$  characteristic), and the potential at which  $I=0$ , respectively. The electron temperature,  $T_e$ , was obtained from the derivative  $\partial(\log I)/\partial V$  in the electron retarding region. The ion density,  $n_i$ , was derived from  $(\partial(I^2)/\partial V)^{1/2}$  in the ion saturation region using the method of Laframboise.<sup>15</sup> The probe was scanned across the chamber allowing the measurement of the plasma parameters as a function of position.

The permanent magnet ECR source generates a highly uniform plasma over diameters  $\sim 300$  mm. Figure 2(a) shows the variation in the  $n_i$ ,  $T_e$ , and  $(V_p - V_f)$  as a function of position in a plane 4 cm above the chuck surface. Measurements were taken in an Ar plasma at 3 mTorr and 2000 W microwave power. The plasma density in the wafer plane is  $\sim 2.5 \times 10^{11}/\text{cm}^3$  with the permanent magnet source. Over a 250 mm diam the uniformity of the plasma parameters is  $< 5\%$ . Uniformity is calculated as  $(\text{max} - \text{min}) / (2 \times \text{mean})$ . The variations in plasma parameters as a function of microwave power in a 5%  $\text{N}_2$  in Ar plasma are shown in Fig. 2(b) and will be discussed in reference to the dependence of the film properties on microwave power in Sec. III C.

### III. RESULTS AND DISCUSSION

Silicon nitride films were deposited using silane, nitrogen, and argon. Nitrogen was injected near the microwave win-

dow and above the ECR resonance zone in Fig. 1(a). Silane was injected in a plane 15 cm above the chuck surface by a system of eight injectors designed to uniformly introduce the gas. Throughout this work, the silane was supplied as a 10% silane in argon mix.

The films were deposited on (100) silicon wafers loaded into the system on an aluminum pallet. Large wafers or arrays of smaller wafers were used to characterize the deposition rate and uniformity over a 300 mm diam. Films were typically deposited to a thickness of  $\sim 100$  nm. The pallet was placed on a cooled chuck maintained at  $20^\circ\text{C}$  with helium gas injected into the gap between the chuck and pallet to enhance heat transfer. Samples were mounted on the pallet using a silver-filled thermally conductive silicone grease. The substrate temperature was measured using Wahl Inst. "temperature dots." During deposition, the wafer surface temperature never exceeded  $100^\circ\text{C}$ .

Following the deposition, the films were characterized as follows. The film thickness and index of refraction were measured with a Gaertner L116 ellipsometer at 632 nm and  $70^\circ$  incidence. The thickness measured by ellipsometry was confirmed by surface profilometry. Film stress was derived from wafer curvature measured before and after deposition using a Tencor Flexus 2320.

The film quality was characterized by an etch rate in a 10:1 buffered oxide etch (BOE) solution (4.5% HF, 35%  $\text{NH}_4\text{F}$  in  $\text{H}_2\text{O}$ ). The film thickness before and after a timed etch was measured by ellipsometry and checked for several samples by surface profilometry. Both methods gave identical results.

Film composition and bonding were evaluated by Fourier-transform infrared (FTIR) spectrometry. Thin films deposited on  $> 10 \Omega\text{cm}$  resistivity,  $p$ -type silicon were evaluated in transmission mode using a Bio-Rad FTS 175. The raw data were subtracted from a bare wafer background and normalized to the peak area of the strong SiN absorption at  $\sim 830 \text{ cm}^{-1}$ . The Si-H absorption has been reported to have an absorption coefficient  $\sim 1.4$  times higher than that of N-H.<sup>16</sup> The areas under the N-H stretch absorption at  $\sim 3340 \text{ cm}^{-1}$  and Si-H stretch at  $\sim 2160 \text{ cm}^{-1}$  were normalized by this factor to arrive at the relative hydrogen content bound at either N-H or Si-H sites and the total hydrogen content.

#### A. Deposition rate and uniformity

Even in a low-density plasma silane is easily dissociated into products with high sticking coefficients.<sup>17,18</sup> The deposition rate depends strongly on the silane flow, as illustrated in Fig. 3 which shows the deposition rate as a function of silane flow. The plotted points are averages at each flow for films deposited at a variety of pressures, microwave powers, and  $\text{N}_2/\text{SiH}_4$  ratios in the course of initial screening experiments and detailed single variable investigations. The magnitude of one standard deviation to the data at each flow is indicated by the error bars. Initial screening experiments established that silane flow has the dominant effect on deposition rate. The effects of pressure, microwave power,  $\text{N}_2$  flow, and their interactions have a much smaller and statistically insignificant effect. In this article we report the effect of

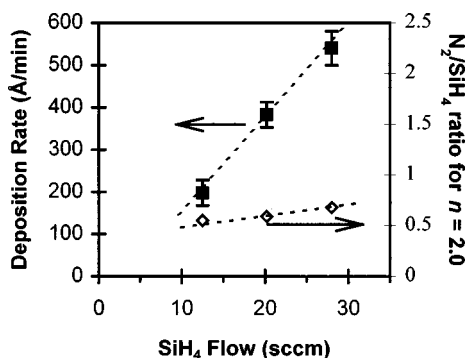


FIG. 3. Deposition rate and  $N_2/SiH_4$  flow ratio required for  $n=2.0$  as a function of silane flow. The  $N_2/SiH_4$  flow ratio results are for films deposited at 4 mTorr chamber pressure and microwave power of 1500 W.

changing the  $N_2/SiH_4$  ratio on film properties for films deposited at deposition rates of 590–680 Å/min with silane flows of 30 sccm in Sec. III B. Section III C contains a detailed discussion of film properties as a function of microwave power and deposition rate. The films discussed in Sec. III C were deposited at 4 mTorr with silane flows of 12.5 and 28 sccm, resulting in deposition rates of  $215 \pm 15$  and  $550 \pm 50$  Å/min, respectively.

Given the high sticking coefficient of the silane decomposition products, the deposition uniformity is primarily determined by the silane gas injection. The injector pattern used in this work provides for a  $1\sigma$  thickness variation of 2.5% over 200 mm and  $\sim 10\%$  over 300 mm diam. Scaling of precursor injection to diameters  $>200$  mm is a relatively straightforward optimization problem.

## B. Nitrogen:silane ratio

The stoichiometry of the deposited film influences a range of materials properties. Index of refraction is often taken as an indicator of film stoichiometry. Stoichiometric thermal nitrides have  $n \sim 2.0$ , Si-rich films  $n > 2$ , and N-rich films  $n < 2$ .<sup>17,19</sup>

Initial screening experiments indicated that the ratio of  $N_2$  to  $SiH_4$  in the source gas has the largest effect on index of refraction. The effect of  $N_2/SiH_4$  on film index of refraction,  $n$ , and etch rate in 10:1 BOE solution is shown in Fig. 4. The microwave power, pressure, and silane flow were held constant at 1200 W, 6 mTorr, and 30 sccm, respectively. Under these conditions the deposition rate is 590–680 Å/min.  $N_2$  flow was varied between 14 and 34 sccm, changing the  $N_2/SiH_4$  ratio from 0.46 to 1.13, and index of refraction,  $n$  from  $\sim 1.7$  to  $\sim 2.5$ . Under these high growth rate conditions, an index of refraction  $n=2.0$  is obtained at a  $N_2/SiH_4$  flow ratio of 0.75.

The  $N_2/SiH_4$  ratio required to deposit  $n=2.0$  films also varies as a function of silane flow as shown on the right axis of Fig. 3 for films deposited at 4 mTorr pressure and 1500 W microwave power. Under these conditions, as the silane flow decreases to 12.5 sccm, the deposition rate decreases to 226 Å/min and the  $N_2/SiH_4$  ratio required for  $n=2.0$  decreases to

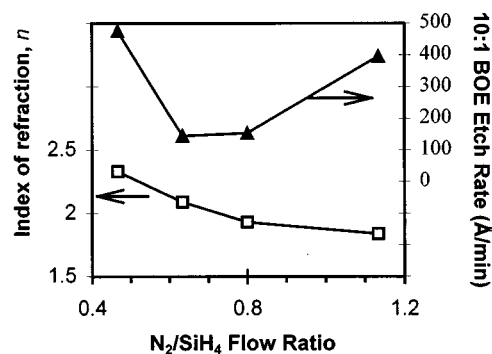


FIG. 4. Index of refraction and etch rate in 10:1 BOE solution as a function of the  $N_2/SiH_4$  ratio. Films were deposited at constant microwave power of 1200 W, pressure of 6 mTorr, and  $SiH_4$  flow of 30 sccm.

0.56. Additional designed experiments indicated that, at a constant  $SiH_4$  flow and  $N_2/SiH_4$ , microwave power and pressure have an insignificant effect on  $n$ .

The etch rate in a 10:1 BOE solution is plotted on the right axis of Fig. 4. A low etch rate is often taken as an indication of high film quality. rf-PECVD nitride films typically have an etch rate  $\sim 500$  Å/min with thermal nitride  $\sim 2$  orders of magnitude lower.<sup>1,17</sup> Here, the BOE etch rate is minimized at  $\sim 150$  Å/min for  $N_2/SiH_4 \sim 0.7$ . The films deposited in this reactor have etch rates between those of thermal nitrides and rf-PECVD films deposited at much higher substrate temperatures.

The variation in film index of refraction as the  $N_2/SiH_4$  flow ratio changes reflects changes in film density, composition, and bonding. Changes in film bonding were investigated by FTIR spectroscopy. Figure 5(a) shows FTIR absorption spectra for the films of Fig. 4. The peaks are identified as follows.<sup>20</sup> The largest absorption peak is the Si–N stretch at  $\sim 830$   $cm^{-1}$ . Hydrogen is indicated by the Si–H and N–H stretch absorption at  $\sim 2160$  and  $\sim 3340$   $cm^{-1}$ , respectively. The N–H bend absorption at  $\sim 1170$   $cm^{-1}$  appears as a shoulder on the large Si–N absorption at  $\sim 830$   $cm^{-1}$ .

The hydrogen content derived from the spectra of Fig. 5(a) is plotted as a function of  $N_2/SiH_4$  in Fig. 5(b). For Si-rich films ( $N_2/SiH_4 < 0.6$ ,  $n > 2$ ), the FTIR spectra indicate very little N–H stretch absorption at  $\sim 3340$   $cm^{-1}$ ; the hydrogen is bound almost exclusively to Si. As the  $N_2/SiH_4$  ratio increases and the index of refraction decreases, the hydrogen bonding shifts from silicon to nitrogen, until at  $N_2/SiH_4 = 1.13$  the Si–H peak has almost completely disappeared. The sum of the signals scaled by the relative absorption coefficient is also plotted in Fig. 5(b). For this microwave power and pressure the total hydrogen content is minimized at a  $N_2/SiH_4$  ratio of  $\sim 0.75$ . Under these conditions  $n=2.0$ .

The FTIR spectra for the  $n=2$  films of Fig. 5 closely resemble those of rf-PECVD films deposited at substrate temperatures  $\sim 350$  °C, although in this case the films are deposited at  $<100$  °C. Elastic recoil detection (ERD) analysis was performed on one sample deposited under similar conditions to the  $n \sim 2$  film of Fig. 4. In this case, the film

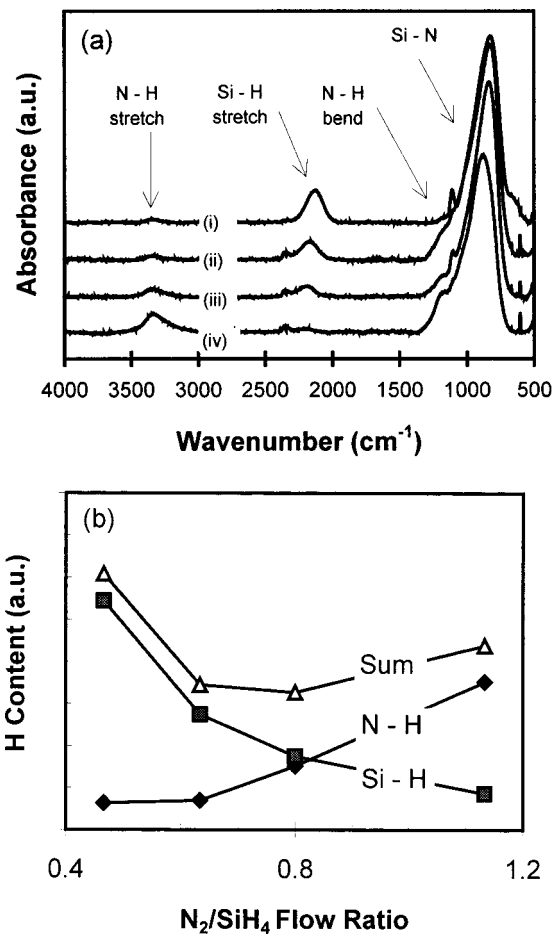


Fig. 5. (a) FTIR absorption spectra of silicon nitride films from Fig. 4. Films were deposited at  $N_2/SiH_4$  ratios of (i) 0.47, (ii) 0.63, (iii) 0.80, and (iv) 1.13. (b) Changes in hydrogen content derived from absorption spectra.

composition was  $\sim 31\%$  Si, 48% N, and 20% H. The hardware configuration used for the ERD sample was an early prototype of the permanent magnet source used in this work. The source used here, however, does not appear to have any fundamental differences, based on film properties such as the BOE etch rate and the dependence of index of refraction on gas flow and composition.

Hydrogen in amorphous silicon nitride films serves to terminate dangling bonds. For rf-PECVD, Smith, Alimonda, and von Pressig<sup>17</sup> have shown that as  $N_2$  flow increases H shifts from terminating dangling Si to terminating dangling N bonds in Si-(NH)-Si complexes. The situation is similar for these low-temperature films, although minimal thermal energy is available at the growth surface to promote chemical condensation reactions.

### C. Microwave power

The high ion current available with this deposition source allows for effective ion-assisted growth. Low-energy ion bombardment can influence film density, microstructure, stress, and composition.<sup>7,9</sup> In addition, the ECR source is

highly efficient at dissociation of molecular nitrogen allowing  $N_2$  to be used in place of ammonia and eliminating one source of hydrogen from the system.

The variation in plasma parameters with microwave power in a 5%  $N_2$  in Ar plasma at 4 mTorr is shown in Fig. 2(b). The most important parameters in this case are the plasma density,  $n_i$ , which largely determines the ion current incident on the wafer, the electron temperature,  $T_e$ , which controls the dissociation rates in the plasma, and the difference between the plasma potential and the floating potential,  $V_p - V_f$ , which is the approximate mean energy of ions reaching the growth surface. The electron temperature and  $V_p - V_f$  remain relatively constant over the microwave power range 750–1500 W, while the plasma density increases by a factor of  $\sim 2.5$ .

Introducing an easily dissociated gas such as silane into the plasma will have a major influence on the plasma equilibrium. Analysis of an Ar/ $N_2$ / $SiH_4$  plasma is difficult, however, due to deposition of an insulating coating on the probe tip. From a simple particle balance perspective,<sup>12</sup> silane additions increase the density of easily dissociated and ionized species and can be expected to decrease  $T_e$ . This would tend to decrease the Ar ionization. Although the plasma parameters plotted in Fig. 2(b) are not quantitatively valid for an actual Ar/ $N_2$ / $SiH_4$  plasma, they should, however, still reflect a qualitative dependence, and function as baseline for comparison to other plasma sources.

Microwave power influences the film properties by activating and dissociating precursors and by providing ions which bombard the growing film. Figure 6 shows the effect of microwave power on stress and the BOE etch rate. Films were deposited with silane flows of 12.5 and 28 sccm at a pressure of 4 mTorr. The  $N_2/SiH_4$  ratio was adjusted to maintain  $n=2.0 \pm 0.02$  where, in reference to Fig. 4, the BOE etch rate is minimized. At low silane flow  $N_2/SiH_4 = 0.56$  leads to  $n=2.0$  films, while at 28 sccm silane flow  $N_2/SiH_4 = 0.70$  is required. At 30 sccm silane flow, as shown in Fig. 4, a still higher  $N_2/SiH_4 \sim 0.75$  is necessary to reach an index of 2.0.

The dependence of stress and the BOE etch rate on the microwave power is sensitive to the silane flow (effective deposition rate). High silane flow is shown in Fig. 6(a). For this set of runs, the deposition rate is  $550 \pm 50 \text{ \AA}/\text{min}$ . At lower microwave powers the film stress is low compressive, and the BOE etch rate is high. As microwave power increases from 750 to 1125 W, the stress increases linearly, while the BOE etch rate drops dramatically, from  $\sim 600$  to  $< 150 \text{ \AA}/\text{min}$ . Above this power, the BOE etch rate saturates at a low value, while stress continues to increase. At lower silane flows, Fig. 6(b), the BOE etch rate is  $< 150 \text{ \AA}/\text{min}$  independent of microwave power, while the compressive stress is higher and retains the linear relationship with the microwave power. The deposition rate in this case is  $215 \pm 15 \text{ \AA}/\text{min}$ .

The effect of changing microwave power on the film IR absorption is plotted in Fig. 7 for films deposited under the high deposition rate conditions of Fig. 6(a). The FTIR spec-

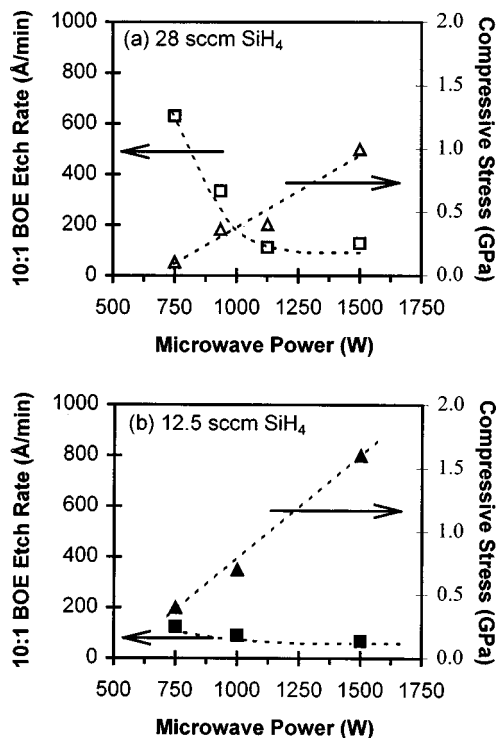


FIG. 6. Effect of microwave power on compressive stress and the BOE etch rate for films deposited at (a) 28 sccm SiH<sub>4</sub>, 550 ± 50 Å/min deposition rate and N<sub>2</sub>/SiH<sub>4</sub> = 0.70 and (b) 12.5 sccm SiH<sub>4</sub>, 215 ± 15 Å/min deposition rate and N<sub>2</sub>/SiH<sub>4</sub> = 0.56. For high SiH<sub>4</sub> flow and deposition rate conditions, low microwave power results in a high BOE etch rate, while at a lower deposition rate, the microwave power has little effect on the BOE etch rate.

tra indicate minimal hydrogen content, consistent with the BOE etch data and stress of Fig. 6(a). The Si–N peak falls at 830 cm<sup>-1</sup>, identical to the value observed for thermal nitride films.<sup>8</sup>

The hydrogen content derived from the spectra of Fig. 7(a) is summarized in Fig. 7(b) as a function of microwave power during deposition. For microwave powers >935 W, the hydrogen content is minimized and independent of the microwave power. At low microwave power the hydrogen content increases by 30%, although the ratio of Si–H to N–H remains constant.

Some minimum ion current to the growth surface is required to fully densify the film. Seaward *et al.* have reported similar results for SiO<sub>2</sub> deposition in an electromagnet ECR system,<sup>7</sup> where high-quality films required a ratio  $J_i/J_0 > 20$  between the ion flux,  $J_i$  estimated from the ion saturation current drawn by a Langmuir probe, and the deposition flux,  $J_0$ , determined from the growth rate. There are large uncertainties inherent in estimating  $J_i/J_0$  for this system, both because plasma diagnostics cannot be done for the exact process plasma, and because of uncertainties in the density and microstructure of the films. Qualitative trends can be evaluated, however, at a deposition rate of 550 Å/min and microwave power of 1500 W  $J_i/J_0 \sim 5$ . At 750 W microwave power,  $J_i/J_0$  decreases to  $\sim 2.5$  as the ion current falls. At a deposition rate of 200 Å/min, the estimate of  $J_i/J_0$  increases from  $\sim 7$  to 14 as the microwave power increases.

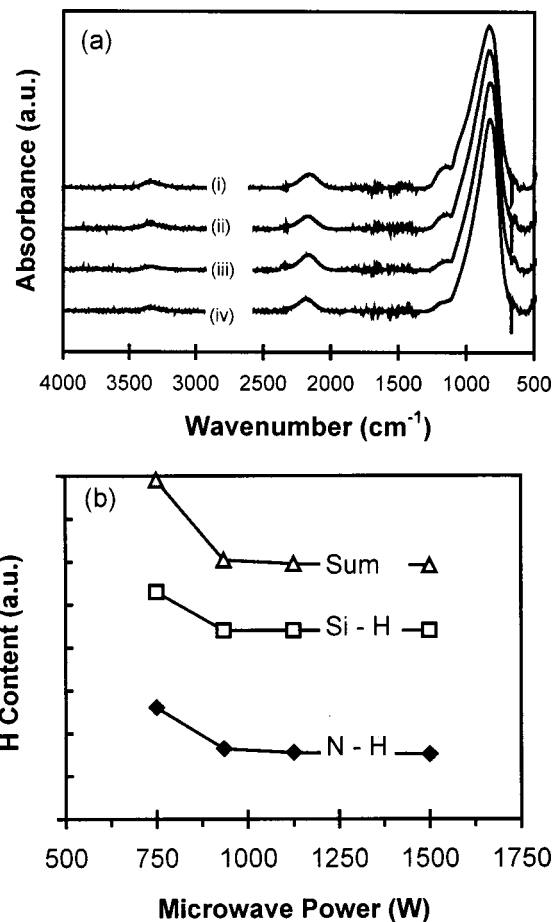


FIG. 7. (a) FTIR absorption of films deposited with 28 sccm SiH<sub>4</sub> flow and microwave powers of (i) 750, (ii) 935, (iii) 1125, and (iv) 1500 W. (b) Changes in hydrogen content derived from absorption spectra as a function of microwave power.

From Fig. 6, a power of  $\sim 1100$  W, and hence,  $J_i/J_0$  estimated at 3.6 is required to deposit a film with a minimal BOE etch rate in this system. The low deposition rate films have  $J_i/J_0 > 7$  over all microwave powers and thus this threshold is not observed. From Fig. 2(b), the mean ion energy,  $e(V_p - V_f)$  is 12 eV, and a minimum of approximately 40 eV/deposited silicon atom is required to produce a film with a low BOE etch rate. Application of rf bias to the substrate during deposition is an alternate method of manipulation of the energy/deposited atom which was not investigated here.

The FTIR data of Fig. 7 indicate little change in the proportion of hydrogen bound at Si–H or N–H sites over the range of microwave power studied. The total hydrogen content decreases by 25% between 750 and 935 W microwave power. The dramatic decrease in the BOE etch rate above  $\sim 1100$  W microwave power illustrated in Fig. 6 relates to both decreasing hydrogen content and increasing film density resulting from increased ion bombardment. This conclusion is consistent with the increase in compressive stress observed at higher microwave powers.

#### IV. CONCLUSIONS

The deposition of silicon nitride at substrate temperatures  $<100^\circ\text{C}$  requires that the thermal energy available at higher substrate temperatures be replaced with bombardment by low energy ions and/or more complete dissociation and activation of the precursors. We have reported silicon nitride deposition in a permanent magnet ECR PECVD reactor. This system is capable of producing a uniform plasma with plasma density  $>10^{11}/\text{cm}^3$  over areas of 300 mm in diameter. The effect of varying process variables on film quality were investigated. This system is capable of depositing low compressive stress ( $<400$  MPa), low 10:1 BOE etch rate, low-hydrogen-content films at substrate temperatures  $<100^\circ\text{C}$ . The dependence of film quality on process variables may be summarized as follows:

(i) The hydrogen content is determined by both the  $\text{N}_2/\text{SiH}_4$  ratio in the feedstock gas and the microwave power. At a deposition rate of 590–680 Å/min and constant microwave power of 1200 W, the hydrogen content is minimized for  $\text{N}_2/\text{SiH}_4 \sim 0.75$ . As the ratio  $\text{N}_2/\text{SiH}_4$  decreases the film index of refraction increases and H moves from N to Si bonding sites.

(ii) As a function of microwave power, the hydrogen content is minimized for powers  $>935$  W for films deposited at rates of  $\sim 550$  Å/min.

(iii) For films deposited at rates of  $\sim 550$  Å/min, a threshold in microwave power of  $\sim 1100$  W exists below which films with high BOE etch rates and low compressive stress are obtained. The threshold corresponds to  $\sim 4$  ions/deposited atom and  $\sim 40$  eV/deposited atom. Above  $\sim 1100$  W microwave power, the BOE etch rate is  $<150$  Å/min and the primary effect of increasing microwave power is to increase film stress.

The low temperature used here allows for deposition on a wide variety of temperature sensitive substrates. Increases of substrate temperature to the  $\sim 300^\circ\text{C}$  range may also allow for a combination of ion-assisted deposition and thermal

chemistry at the growth surface. This might allow for deposition of nitrides with very low hydrogen content and gate quality dielectric properties. The electronic properties of these nitrides will be the subject of future investigation.

<sup>1</sup>S. K. Ghandhi, *VLSI Fabrication Principles* (Wiley, New York, 1994), pp. 510–578.

<sup>2</sup>W. L. Gardner and M. Dalvie, American Vacuum Society National Symposium, San Jose CA, 1997 (unpublished); H. Chatam, *Surf. Coat. Technol.* **78**, 128 (1996).

<sup>3</sup>Y. Ma, T. Yasuda, and G. Lucovsky, *J. Vac. Sci. Technol. A* **11**, 952 (1993); Y. Ma, T. Yasuda, and G. Lucovsky, *Appl. Phys. Lett.* **64**, 2226 (1994); I. Kato, K. Naguchi, and K. Numada, *J. Appl. Phys.* **62**, 492 (1987).

<sup>4</sup>X. Wang, T.-P. Ma, G.-G. Cui, T. Tamagawa, J. W. Goltz, S. Karechi, B. H. Halpern, and J. J. Schmidt, *Jpn. J. Appl. Phys., Part 1* **34**, 955 (1995).

<sup>5</sup>H. Arai, K. Tanaka, and S. Kohda, *J. Vac. Sci. Technol. B* **6**, 831 (1988).

<sup>6</sup>J. C. Barbour, H. J. Stein, and C. A. Outten, *J. Vac. Sci. Technol. A* **9**, 480 (1991); K. Machida, T. Hosoya, K. Imai, and E. Arai, *J. Vac. Sci. Technol. B* **13**, 876 (1995); S. W. Matsuo and M. Kiuchi, *Jpn. J. Appl. Phys., Part 2* **22**, L210 (1983); M. J. Hernandez, J. Garrido, J. Martinez, and J. Piqueras, *J. Electrochem. Soc.* **141**, 3234 (1994).

<sup>7</sup>K. L. Seaward, J. E. Turner, K. Nauka, and A. M. E. Nel, *J. Vac. Sci. Technol. B* **13**, 118 (1995).

<sup>8</sup>S. Sitbon, M. C. Hugon, B. Aguis, F. Abel, J. L. Courant, and M. Puech, *J. Vac. Sci. Technol. A* **13**, 2900 (1995).

<sup>9</sup>J. S. Colligon, *J. Vac. Sci. Technol. A* **13**, 1649 (1995).

<sup>10</sup>T. Mantei, U. S. Patent No. 5,196,670.

<sup>11</sup>J. E. Stevens, in *High-Density Plasma Sources*, edited by O. A. Popov (Noyes, Park Ridge, NJ, 1995), p. 312.

<sup>12</sup>M. A. Lieberman and A. J. Lichtenberg, *Principles of Plasma Discharges and Materials Processing* (Wiley, New York, 1994), pp. 19–22, 515.

<sup>13</sup>*Handbook of Chemistry and Physics* (CRC Press, Boca Raton, 1994), pp. 9–55.

<sup>14</sup>A. Saproo and T. D. Mantei, *J. Vac. Sci. Technol. A* **13**, 883 (1995).

<sup>15</sup>J. G. Lafromboise, UTIAS Report No. 100, University of Toronto (1966).

<sup>16</sup>W. A. Langford and M. J. Rand, *J. Appl. Phys.* **49**, 2473 (1978).

<sup>17</sup>D. L. Smith, A. S. Alimonda, and F. J. von Pressig, *J. Vac. Sci. Technol. B* **8**, 551 (1990).

<sup>18</sup>D. L. Smith, *J. Vac. Sci. Technol. A* **11**, 1843 (1993).

<sup>19</sup>T. E. Wagy, C. D. Fung, and W. H. Ko, *Silicon Nitride Thin Insulating Films*, edited by V. J. Kapoor and H. J. Stein (The Electrochemical Society, Pennington, NJ, 1983), p. 167.

<sup>20</sup>S. E. Alexandrov and M. L. Hitchman, *Chem. Vap. Deposition* **3**, 111 (1997); W. R. Knolle and J. W. Osenbach, *J. Appl. Phys.* **58**, 248 (1985); J. P. Luongo, *Appl. Spectrosc.* **38**, 195 (1984).